Journal of Operation and Automation in Power Engineering

vol. XX, no. XX, Dec. 2022, Pages: XXXX (Proofed)

http://joape.uma.ac.ir

Islanding Detection of Synchronous Generator in Distribution Network Based on Machine Learning Methods

M. Khodsuz[*]

Faculty of Electrical and Computer Engineering, University of Science and Technology of Mazandaran, Behshahr, Mazandaran, Iran.

Abstract— *In this paper, a novel approach for detecting islanding events in distribution networks special for synchronous generator type is presented. The proposed method leverages information derived from negative sequence voltage components, synchronous generator field voltage, positive sequence impedance variation rate, voltage harmonic distortion factor, and features extracted through wavelet transform applied to voltage waveforms. In order to establish a robust classification system without the necessity of explicit threshold determination, a pattern recognition method is employed. The dataset derived from these characteristics undergoes training using multi-layer support vector machines and a random forest optimization algorithm, resulting in five distinct classes. The study incorporates experimental samples encompassing various scenarios such as symmetric and asymmetric fault occurrences, load variations at different points, capacitor bank switching, variable load switching, nonlinear load switching, and islanding on a modified 34-bus IEEE network. The proposed islanding detection method demonstrates its effectiveness in distinguishing electrical islanding from power quality phenomena such as voltage oscillation, voltage sag, voltage swell, and dynamic voltage changes. Conducted simulations in MATLAB validate the efficacy of the proposed method.*

Keywords—Islanding detection, synchronous generator, support vector machines, rendom forest, power quality phenomena.

1. INTRODUCTION

With the increasing daily consumption of electrical energy, achieving methods for rapid energy supply and ensuring consumer satisfaction are the most important objectives for power network. This trend has led to the design of power generation sources with limited capacity capable of connecting to the distribution network or consumers. One of the phenomena that constantly encounters with the installation of distributed generation (DG) in the distribution network is the islanding of distributed generation sources. Given the high significance of this phenomenon, the IEEE 929 standard, published in 1988, addressed the need to disconnect distributed generation. Recognizing the operational necessity in the presence of islanding, the IEEE 1547 standard was introduced in 2003, proposing a maximum time of 2 seconds for islanding detection. The presence of electrical islanding consistently exerts notable influences on the distribution network, with alterations in protective measures standing out as one of the pivotal consequences. Given the considerable expenses associated with power network equipment, the primary measure in safeguarding the distribution network against the influence of distributed generation sources involves identifying electrical islands. Diverse techniques have been suggested for islanding detection, broadly classified into two groups: remote and local methods. Remote islanding detection methods rely on communication between the network and distributed generation. Despite offering higher reliability compared to local detection methods, the widespread adoption of this approach has been hindered by its high cost and lack of economic feasibility [1–5].

Local islanding detection methods operate based on measuring network parameters at the DG location. This method is divided into three categories: passive, active, and hybrid methods. The passive method, which is also the focus of this article, operates based on measuring network parameters and does not disturb the operation of DG [6–9]. Voltage magnitude at the distributed generation terminal, DG output power fluctuations, frequency monitoring and impedance variation are some of the proposed methods for passive islanding detection. Factors that pose challenges to passive islanding detection include the use of parameter-based methods, threshold determination for parameter detection, and the balance between production and consumption in the islanding zone. The threshold values will undergo changes due to variations in local and remote loads, and many of the parameters used in detection depend on the balance between load and generation. In case of an imbalance, these parameters may not exceed their threshold values, leading to incorrect islanding detection. In addition, events such as capacitor bank switching, symmetric and asymmetric faults, variable and nonlinear load switching may introduce variations in detection parameters, similar to what occurs during islanding. Such conditions can result in the failure of proper islanding detection [10–16]. The local methods for islanding detection can be categorized into three sets: passive (one-site), active, and hybrid methods. Passive methods rely on measuring various network parameters at the point of common coupling (PCC) [17], including under-voltage, under-current protection, rate of change of frequency (ROCOF) [18], rate of change of angle difference, vector shift, rate of change of voltage, and voltage and current harmonics [19, 20]. Active methods involve manipulating signals at the PCC, intentionally misaligning them to detect islanding operation modes. These methods prove effective during islanded operations due to significant changes in electrical parameters at the PCC. However, they may compromise energy quality at distributed generation and PCC buses in distribution networks [21, 22]. Certain active methods use signal impulse and high-frequency signal injection, reactive-power control, current injection, harmonic

Received: 27 Dec. 2023
Revised: 23 Jan. 2024
Accepted: 31 Jan. 2024
[*]Corresponding author:
E-mail: m.khodsouz@mazust.ac.ir (M. Khodsuz)
DOI: 10.22098/joape.2024.14318.2100
Research Paper

drifting, adaptive active current disturbance, active phase shift, active frequency drift, and Sandia frequency shift. Hybrid methods combine features of both active and passive approaches. Notably, recent islanding-detection methods primarily leverage artificial intelligence (AI) techniques such as artificial neural networks (ANN), adaptive neuro-fuzzy inference system (ANFIS), and decision trees. These noninvasive AI-based methods boast a quick detection period of less than 60 ms without causing disturbances or impacting power quality at the PCC [23, 24]. However, despite their advantages, AI-based techniques require significant time for learning and testing, making them time-consuming. Consequently, these methods have yet to find applications in commercially available numeric relays for hardware solutions, especially in DG relays analyzed for anti-islanding protection. While some methods align closely with previously presented approaches, there remains a lack of integration into the market for numeric relays [25].

In this article, a passive method for islanding detection and its differentiation from power quality phenomena resulting from symmetric and asymmetric faults, capacitor bank switching, variable load, and nonlinear load for distributed synchronous generator is proposed. This method is based on characteristics such as negative sequence voltage component, synchronous generator field voltage, positive sequence impedance rate variation, harmonic distortion factor deviation, and features extracted from wavelet transform of voltage waveforms. Pattern recognition techniques, such as support vector machines (SVMs) and random forest (RF), are employed to distinguish between islanding and non-islanding states using data collected from the mentioned characteristics in various experiments conducted on a modified 34-bus IEEE distribution network. Multi-layer Support Vector Machines and also random forest classification algorithm are utilized to classify distribution network variation in five stages.

In the subsequent sections of the article, the network model under investigation is presented, followed by the introduction of the architecture of the multi-layer support vector machine and random forest in Section 3. Parameters used in passive islanding detection for synchronous generator productions are examined in Section 4, and the proposed method is detailed in Section 5. Simulation results are presented in Section 6, and the conclusions are summarized in Section 7.

2. The System Modeling

In this article, the proposed islanding detection method is evaluated using the modified 34-bus IEEE distribution network operating at a frequency of 60Hz [4, 5]. Two distributed synchronous generators, as illustrated in Fig. 1, are considered for this network. These generators have production capacities of DG1=5MVA and DG2=2.5MVA.

The base loads for each distributed generation are depicted in the figure. To examine the impact of load changes at the terminal of each distributed generation, loads LL-1 and LL-2 are varied. Additionally, to investigate the effect of capacitor bank switching, capacitors C1 and C2 are switched on in the subnetworks 1 and 2, respectively. Moreover, external load EL will be switched at point 806. In this network, the nonlinear load, voltage notch (Notch) generator, is connected at points 810 and 856. Also, the variable load for generating voltage oscillations (Voltage Unbalance) is connected to these points. To examine the effects of symmetric and asymmetric faults, a lightning model is utilized at point 806 for a duration of 0.2 seconds. Islanding conditions in this network are induced by opening the switches at points 806, 810, and 856, and measurements will be taken at the terminals of both DGs.

3. Optimization Algorithm

3.1. Multi-layer support vector machine architecture

To separate N groups of information using a Multi SVM classifier, N-1 stages of separation are required. In this method,

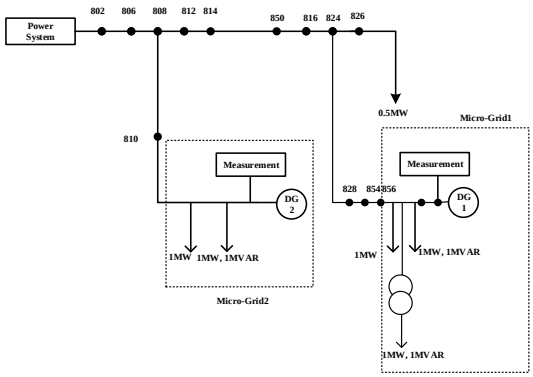

Fig. 1. 34-Bus IEEE improved distribution system.

Table 1. The implemented parameters of the SVM.

Parameter	Description	Value
Train set size	The size of the training set	60%
Validation set size	The size of test set	40%
C	Regularization parameter. The strength of the regularization is inversely proportional to C	1.5
Kernel	Specifies the kernel type to be used in the algorithm	Radial basis function
Gamma	Kernel coefficient for 'rbf'	Auto
Max iterint	Hard limit on iterations within solver	No limit
Random stateint	Controls the pseudo random number generation for shuffling the data for probability estimates	True
Normalization	Normalization of input data in the range of -1 to 1	True

the training and testing process for three classification stages is performed similarly, as shown in Fig. 2 [26]. Information from the first category is separated from the total information using SVM1, and SVM2 separates information from the second category from the remaining information. The remaining information at this stage represents the third category. Given the potential for non-identification of data associated with a class at each stage of data classification, the described approach will result in a certain quantity of data in the final class remaining unallocated throughout the SVM data classification procedure. To address this issue and enhance classification reliability, preventing the impact of uncategorized information on other classes, modifications have been made to the architecture of the multi-layer Support Vector Machine for both training data and test data [27]. Table 1 enumerates some of the implemented parameters of the SVM.

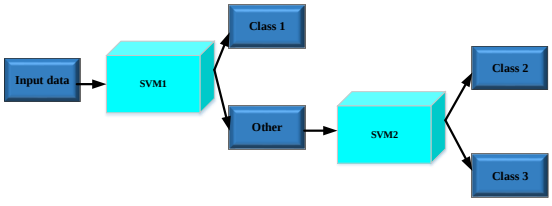

Fig. 2. The training and testing process for three classification stages.

3.2. Random forest opmization algorithm

RF represents a hybrid learning approach applicable to both classification and regression tasks, relying on a framework composed of numerous decision trees. Specifically, effective for decision trees prone to overfitting the training set, RF typically outperforms individual decision trees. However, the extent of

Table 2. The characteristic of RF parameters.

Parameter	Description	Value
Number of estimators	The number of trees in the forest	200
Criterion	The function to measure the quality of a split	Gini
Train set size	The size of the training set	60%
Validation set size	The size of test set	40%
Max depth	The maximum depth of the tree	6
Min samples split	The minimum number of samples required to split an internal node	2
Min samples leaf	The minimum number of samples required to be at a leaf node	2
Features max	The number of features to consider when looking for the best split	None

performance enhancement varies depending on the data type. Instead of depending on a singular decision tree, a random forest predicts outcomes from each tree, aggregates the majority of votes, and deems the consolidated result as the output. Increased tree quantity in the forest enhances accuracy and mitigates overfitting [28]. Notably, this algorithm operates independently of specific parameters in machine learning. In constructing a random forest classifier, features are randomly selected for each tree, introducing variability in the decision mapping for each. Every decision tree involves a random subset of samples, chosen with replacement from the training dataset, allowing each tree to potentially use an entirely distinct set of data points. The characteristics of the RF utilized in this manuscript are detailed in Table 2. In addition, the RF flowchart has been shown in Fig. 3.

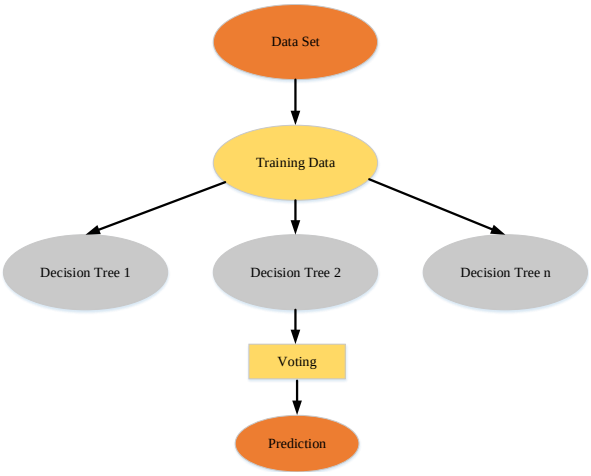

Fig. 3. The RF classifier flowchart.

4. Investigation of Islanding Detection Parameters

The distribution network experiences varying load levels determined by the connected loads. Changes in the network, such as load connections/disconnections, symmetric/asymmetric faults, and islanding, occur based on the network loading, leading to similar impacts on voltage and current. Consequently, developing a reliable indicator capable of effectively discerning electrical islands from other network changes proves challenging. Addressing this requirement, the adoption of a multi-criteria passive method becomes essential for establishing a dependable and efficient approach.

4.1. Negative sequence voltage component

Due to the diverse changes introduced by the presence of distributed generation sources, network symmetry is consistently disrupted. The occurrence of asymmetric faults, capacitor bank switching, variable load switching, islanding, and other factors result in changes to voltage magnitude and phase, depending on the size of the equipment being switched. This phenomenon contributes to the creation of voltage imbalance, which, in turn, is the cause of the appearance of the negative sequence voltage component.

According to Fig. 4, the occurrence of an electrical island takes place at a specific moment. As illustrated in Fig. 4, the magnitude and phase of the voltage waveform has been changed during islanding. The magnitude of negative sequence voltage during islanding is highly dependent on the balance between load and dependent generation; thus, it is not a suitable parameter for detection. However, the modulation of this parameter during islanding has been utilized as a detection factor in this paper. In reference [9], for achieving a fast islanding detection method for distributed generation based on the inverter, injecting negative sequence current and examining the modulation trend of negative sequence voltage have been employed.

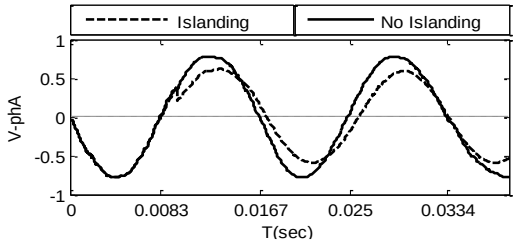

Fig. 4. The variation of amplitude and phase angle of voltage during islanding.

The utilization of this parameter stems from the inherent ability of the synchronous generator to generate negative sequence current. The fluctuations in negative sequence voltage, as illustrated in Fig. 5 for islanded, load connection, and capacitor bank connection scenarios, are demonstrated. It is noticeable that, owing to islanding, the value of this parameter consistently surpasses the threshold level.

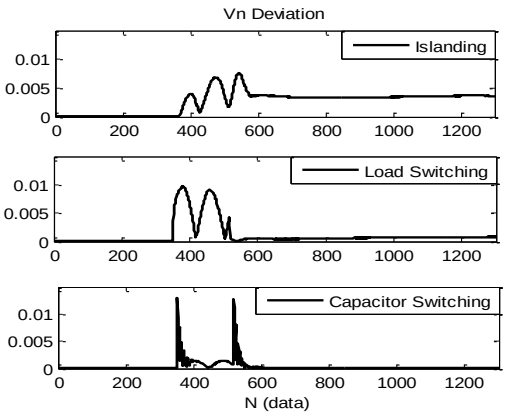

Fig. 5. The variation of negative sequence voltage during islanding load connection, and capacitor bank connection.

4.2. Generator field voltage

Symmetric and asymmetric faults in the network produces alterations in the proposed detection parameters, surpassing the defined islanding threshold. The capability to identify network faults and differentiate them from other factors impacting detection parameters aids in the passive method of islanding detection.

To realize this objective, the field voltage of the synchronous generator is employed. The control system for generator excitation, developed in MATLAB software, follows the IEEE 421.5 standard from 1992.

The fundamental elements in the excitation system are the voltage regulator and the exciter. The exciter establishes a relationship between the exciter field voltage (V_{fd}) and the output of the voltage regulator (e_f) using the transformation function provided in Eq. (1).

$$\frac{V_{fd}}{e_f} = \frac{1}{K_e + sT_e}. \tag{1}$$

Since the generator field is supplied by the excitation field voltage, the generator field voltage is utilized to distinguish faults from other network variations. In the event of a fault in the network, the generator terminal voltage (V_t) experiences a significant drop, causing a sudden increase in the fault voltage according to Eq. (2).

$$V_{error} = V_{ref} - V_t. \tag{2}$$

In this relation, V_{ref} is considered 1 perunit. The fault voltage signal is sent to the exciter to compensate for the generator's output voltage. Given the high gain of the voltage regulator, it increases its input. The signal e_f from the regulator output, according to Eq. (1), will abruptly increase the excitation field voltage. Such abrupt variations lead to an instantaneous increase in the excitation current, but due to the inductive property of the system, the instantaneous change in excitation current is not feasible. Fig. 6 illustrates the effect of network changes such as switching of load LL-1 at 1s and 2s, load EL switching at the time 3s and 4s, capacitor bank switching at 5s and 6s, and three-phase fault at the time equal to 7s on the excitation field voltage. As seen in the figure, the proposed parameter achieves satisfactory performance during the fault occurrence.

As long as a fault exists in the network, V_{fd} remains upper than the threshold. With fault clearance, in contrast to the previous condition, V_{fd} suddenly increases, leading to a reduction, and proportionally, a decrease in the excitation current.

4.3. Positive sequence impedance variation rate

As depicted in Fig. 7, one of the most significant changes that follows the deviation trend of negative sequence voltage, similar to the occurrence of an island, is the connection of a variable load. For variable load simulation the variable load block in MATLAb software has been implemented. Since the voltage exhibits oscillatory behavior, the negative sequence voltage component arises due to voltage oscillation. Consequently, separating these conditions from islanding is crucial. To distinguish the variable load connection from other network changes, the positive sequence impedance rate of change has been utilized. Given the variable nature of the voltage magnitude, the positive sequence impedance rate of change achieves the most significant impact.

4.4. Harmonic distortion factor

Distributed generation outputs play a significant role in generating voltage harmonics, depending on their technology. Distributed generation sources connected to the grid through power electronic converters have garnered much attention among other distributed generation technologies due to the switching actions performed in these converters. Synchronous generators also produce voltage harmonics due to the nonsinusoidal distribution of flux in their windings. Additionally, the flux resulting from the creation of negative sequence current in this type of distributed generation produces third-order harmonic.

Several measurement methods exist to illustrate the magnitude and size of harmonics in a waveform by a single number. One

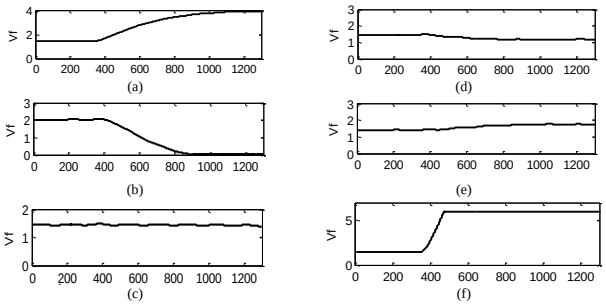

Fig. 6. The Effect of fault on detection parameter (a) Load connection in micro-grid 1 (b) Load disconnection in micro-grid 1 (c) Load disconnection in micro-grid 2 (d) Capacitor bank connection in micro-grid 1 (e) Capacitor bank disconnection in micro-grid 1 (f) 3phases fault.

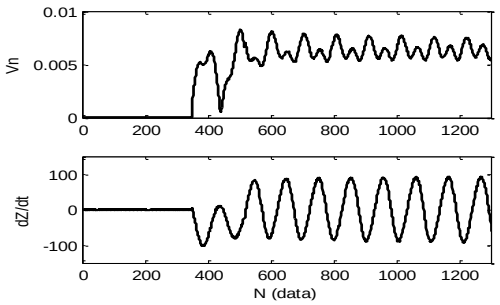

Fig. 7. The variation of the negative sequence voltage and the positive sequence impedance of variable load.

of the most common methods is the Total Harmonic Distortion (THD), which can be obtained for voltage or current according to Eq. (3).

$$THDv = \left(\sqrt{\sum_{h=2}^{N} V_h^2} \Big/ V1 \right) \times 100. \tag{3}$$

To calculate THD, it is necessary that the voltage waveform to be in a stable state. This is challenging as any change in the network alters the fundamental frequency. Therefore, calculating THD seems impractical. To examine the harmonic variations resulting from islanding and other factors affecting the voltage waveform, it is assumed that the fundamental frequency component remains constant with any frequency variation.

In the case of connecting DG to the network, voltage quality control at the common point of connection between DG and the network is the responsibility of the network. Additionally, under normal conditions when DG is connected to the network, the equivalent impedance from the DG terminal is very small. Given that harmonic components always exist in a very small range compared to the main component in terms of amplitude, the current drawn by the load for these components will also be negligible. Therefore, the harmonic distortion factor of the voltage will allocate a small amount.

In the event of islanding, the synchronous generator generates low-order harmonics, causing a delay in the damping of harmonic components. Simultaneously, the creation of an island results in a sudden increase in the equivalent impedance from the DG terminal. Observing the changes in impedance and current trends, the amplitude of voltage harmonic components rises, consequently elevating the Total Harmonic Distortion. Fig. 8 depicts the trend of THD variation of three scenarios: islanding, connecting a capacitor bank, and load connecting.

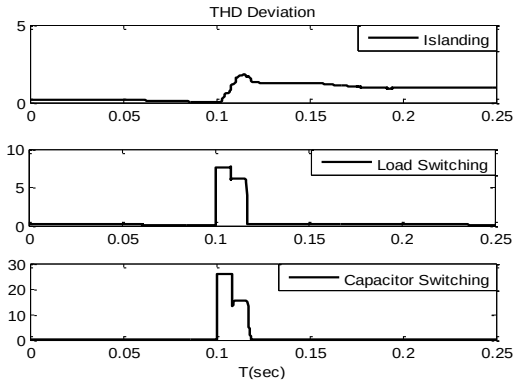

Fig. 8. THD changes due to islanding, load connection and capacitor bank connection.

Table 3. The test numbers and variation for collecting dataset.

Variation Type	Test numbers	Test Percent
Load connection and disconnection in DG-1,2	648	40
Capacitive bank connection and disconnection in DG-1,2	324	20
Linear load connection and disconnection in G-1,2	54	3/33
Non-Linear load connection and disconnection in G-1,2	54	3/13
Fault in 806	135	8/33
Islanding	405	25

4.5. Extracted wavelet transform indices

In order to utilize wavelet transform for islanding detection, the second-level decomposition has been employed. Under various network loading conditions, each parameter provides a wide range of variations. For certain changes, especially load interruptions, the obtained results and islanding scenarios will be very similar. By examining the $Detail-2$ results from $db2$, conditions for circuit breaker (CB) disconnecting can be determined for each type of network change using the domain value. Since islanding occurs due to CB disconnects, the electrical islanding will be distinguished from all separate CB connection conditions using this parameter [29]. Another extracted index is the energy and the amplitude of the wavelet transform.

5. Proposed Method

The separation of electrical islanding from power quality phenomena in this article is based on examining the effects of network variations on voltage and current and determining an index that distinctly identifies these changes from islanding. The possible network-induced changes and their influential effects are presented in Table 3.

The use of pattern recognition methods requires data for training. To obtain the necessary information in this article, numerous experiments have been conducted on the examined network. Table 1 shows the number of these experiments for each network variation.

Baseline loads of (0.5 MW, 0.5 MVAr), (1 MW, 1 MVAr), and (1.5 MW, 1.5 MVAr) have been defined for each distributed generation (DG). Consequently, the combination of possible conditions for two DGs results in 9 different base loading states for the network. To investigate the effect of the CB -switching angle on the parameters of interest, three angles (0, 45, and 90 degrees) have been considered for both open and closed CB states for each experiment. The examination of the CB -switching angle under CB disconnecting conditions, considering the CB closing at the zero current crossing point, is crucial due to the calculations performed in the wavelet transform. Since, as a result of disconnecting one phase, the other phase may reach its zero current crossing point sooner and disconnect, various transient states occur, leading to changes in the output of the wavelet transform.

In the context of load switching at the terminal of each DG, six loads of different magnitudes have been considered. These loads correspond to %30, %50, %70, %90, %100, %120, and %150 of the baseline load (1 MW, 1 MVAr). This range of load variations has been utilized to examine various conditions of balance between load and generation for islanding scenarios. The obtained data for islanding scenarios are derived from creating islands at three points: 806, 856, and 810. In the analysis of each distributed generation, the data related to islanding include the DG itself and the islanding of DG-1,2. Fig. 9 illustrates the algorithm of the proposed method.

Determining the threshold values for inactive detection parameters, which are among the most important and challenging parts of the configuration of these methods, has given way to a classification-based approach. The nine parameters have been defined as inputs to the Multi SVM. These parameters include the synchronous generator field voltage, the magnitude and phase of the negative sequence voltage, the magnitude and phase of the positive sequence impedance rate, the deviation of the voltage harmonic distortion factor, magnitude and energy. A total of 1620 training data are obtained. The indices used in the proposed method are divided into two categories: transient and super-transient indices.

The synchronous generator field voltage (a), the negative sequence voltage magnitude (b), the positive sequence impedance rate magnitude (c), the $Detail-2$ magnitude (d), and the $Detail-2$ energy (e), which utilize information from the transient cycle for calculations, are referred to as transient indices. The negative sequence voltage magnitude (f), the positive sequence impedance rate magnitude (g), and the harmonic distortion factor deviation (h), which utilize information from two cycles after the transient cycle, are recognized as super-transient indices in this article. Fig. 10 illustrates the positions of three parameters, the $Detail-2$ voltage waveform, synchronous generator field voltage, and positive sequence impedance rate magnitude, versus on the magnitude of the negative sequence voltage as an example for two islanding and non-islanding states.

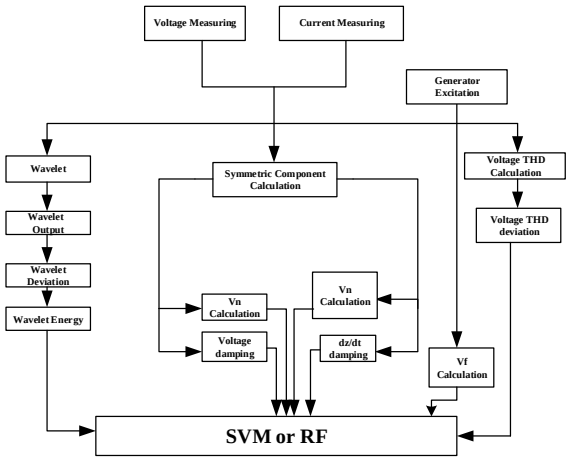

Fig. 9. The proposed algorithm.

6. Results and Simulation

By the information obtained from transient and super-transient indices, to evaluate the proposed method, the dataset is divided into two categories: training and testing samples. The SVM used in this simulation for distinguishing five islanding states, voltage sag, voltage fluctuation, voltage dynamic increase, and decrease, is composed of five layers according to the proposed architecture pattern in [27]. In the training process of SVM1, as shown in Fig. 2, this network learns from the entire information for the separation of the first group from the rest.

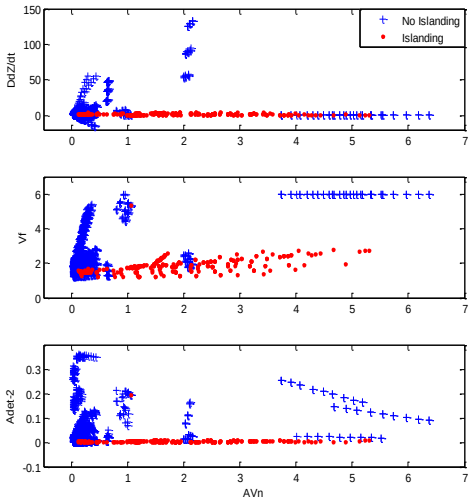

Fig. 10. Result of islanding and non-islanding.

Table 4. SVM classification results accuracy.

		SVM1	SVM2
Non-linear	Polynomial	82.8	82.2
	MLP	85.9	81.5
	RBF	89.1	87.4
Linear		87.6	86.3

Based on this, SVM2, SVM3, SVM4, and SVM5 are trained separately for the second, third, fourth, and fifth groups, respectively, using all the data. To perform experiments on the trained networks, the remaining 40% of the data will be used. In the first stage of separation, testing samples related to voltage sag will be separated from other samples. In the second stage, SVM2 isolates voltage fluctuation as another power quality phenomenon from the testing data. In the third stage, the separation of voltage dynamic increase will be considered, and based on this, SVM3 performs this task. If the pattern in [27] is used in this simulation, SVM4 is considered the last step, which separates voltage dynamic decrease and islanding from each other. However, the samples that have not obtained their desired class in the three previous stages will be placed in the islanding class, reducing the accuracy of islanding data classification. To increase the reliability of the data separation method, SVM5 is used. Thus, conditions are provided to eliminate samples that have been transferred from the first layer to the final layer. Table 4 shows the information obtained from the classification of data into five desired classes for linear and nonlinear support vector machines with RBF, MLP, and polynomial kernel functions. As seen, the RBF support vector machine is capable of effectively distinguishing islanding from other power quality phenomena.

In this condition, the accuracy of the RF was 93.21% which shawn that this classifier was able to diagnose the islanding condition better than the SVM.

For a more in-depth examination of the proposed criteria, an extensive analysis has been conducted using various metrics, including recall, precision, and F1-score, across different considered classifiers. Recall assesses the model's capability to correctly identify true positives, also referred to as the true positive rate. It is computed by dividing true positives by the sum of true positives and false negatives. Conversely, precision represents the ratio of true positives to all points classified as positives, requiring positive and negative numbers from the confusion matrix for its calculation. The F1-score serves as the harmonic mean of precision and recall. The computation of these indices is outlined below:

Table 5. The performance of classifiers with various feature combinations with proposed criteria.

Classifier	Accuracy(%)	Precision(%)	Recall(%)	F_1(%)
RF	93.21	92.15	90.25	91.19
SVM-RBF	89.1	89.85	88.35	89.09

$$\begin{aligned} \text{Precision} &= \frac{TP}{TP+FP} \\ \text{Recall} &= \frac{TP}{TP+FN} \\ F_1 &= 2 * \frac{\text{Recall}*\text{Precision}}{\text{Recall}+\text{Precision}}. \end{aligned} \tag{4}$$

where TP is the true positive, FP is the false positive, and FN is the false negative.

The results of incorporating these feature combinations into various classification models have been represented in Table 5.

7. CONCLUSION

This article introduces a novel method aimed at distinguishing islanding from power quality phenomena, including voltage sag, fluctuation, dynamic increase, and decrease, within a distribution network. The classification of test data is achieved using SVM and RF classifiers. Information essential for the method is derived from the negative sequence component of voltage, synchronous generator field voltage, positive sequence impedance ratevariation, voltage harmonic distortion coefficient, and features extracted from the wavelet transform of voltage waveform. A comprehensive dataset comprising 1620 different scenarios is tested on the 34-bus IEEE network for data collection. The training and testing data, processed by the multilayer support vector machine, are segregated into five stages. The proposed parameters demonstrate satisfactory performance in islanding conditions, encompassing various load-switching scenarios, capacitor bank switching, three-phase faults, two-phase faults, single-phase faults, and variable and nonlinear load switching. The obtained results are:

- The RBF kernel accurately distinguishes the islanding state from power quality phenomena with high precision compared to the MLP and linear SVM. The accuracy of the RBF was 89.1% whereas the accuracy of linear and MLP were 87.6% and 85.9%, respectively.
- Comparing the RF and SVM algorithms shown thet the RF efficiency is higher than the SVM for islanding detection. The accuracy of RF was 93.21%.
- The recall and F1 score of the RF optimizer were 90.25% and 91.19% and these values for SVM were 88.35% and 89.09%, respectively.

REFERENCES

[1] M. Seyedi, S. A. Taher, B. Ganji, and J. Guerrero, "A hybrid islanding detection method based on the rates of changes in voltage and active power for the multi-inverter systems," *IEEE Trans. Smart Grid*, vol. 12, no. 4, pp. 2800–2811, 2021.

[2] A. Hussain, C.-H. Kim, and S. Admasie, "An intelligent islanding detection of distribution networks with synchronous machine dg using ensemble learning and canonical methods," *IET Gener. Transm. Distrib.*, vol. 15, no. 23, pp. 3242–3255, 2021.

[3] H. Radmanesh and M. Saeidi, "Stabilizing microgrid frequency by linear controller design to increase dynamic response of diesel generator frequency control loop," *J. Oper. Autom. Power Eng.*, vol. 7, no. 2, pp. 216–226, 2019.

[4] "Ieee recommended practice for utility interface of photovoltaic (pv) systems," *IEEE Std 929-2000*, 2000.

[5] I. Sepehrirad, R. Ebrahimi, E. Alibeiki, and S. Ranjbar, "Thevenin impedance concept for fast detection of microgrid

islanding scenarios in the presence of small synchronous generators," *J. Oper. Autom. Power Eng.*, vol. 12, no. 2, pp. 91–106, 2024.

[6] A. Khamis, H. Shareef, E. Bizkevelci, and T. Khatib, "A review of islanding detection techniques for renewable distributed generation systems," *Renewable Sustainable Energy Rev.*, vol. 28, pp. 483–493, 2013.

[7] R. Bakhshi-Jafarabadi, J. Sadeh, J. de Jesus Chavez, and M. Popov, "Two-level islanding detection method for grid-connected photovoltaic system-based microgrid with small non-detection zone," *IEEE Trans. Smart Grid*, vol. 12, no. 2, pp. 1063–1072, 2020.

[8] D. Mlakić, H. R. Baghaee, and S. Nikolovski, "A novel anfis-based islanding detection for inverter-interfaced microgrids," *IEEE Trans. Smart Grid*, vol. 10, no. 4, pp. 4411–4424, 2018.

[9] J. C. Vieira, W. Freitas, and D. Salles, "Characteristics of voltage relays for embedded synchronous generators protection," *IET Gener. Transm. Distrib.*, vol. 1, no. 3, pp. 484–491, 2007.

[10] B. Pangedaiah, P. S. K. Reddy, Y. Obulesu, V. R. Kota, and M. L. Alghaythi, "A robust passive islanding detection technique with zero-non-detection zone for inverter-interfaced distributed generation," *IEEE Access*, vol. 10, pp. 96296–96306, 2022.

[11] A. Rostami, H. Abdi, M. Moradi, J. Olamaei, and E. Naderi, "Islanding detection based on rocov and rocorp parameters in the presence of synchronous dg applying the capacitor connection strategy," *Electr. Power Compon. Syst.*, vol. 45, no. 3, pp. 315–330, 2017.

[12] H. R. Baghaee, D. Mlakić, S. Nikolovski, and T. Dragicević, "Support vector machine-based islanding and grid fault detection in active distribution networks," *IEEE J. Emerging Sel. Top. Power Electron.*, vol. 8, no. 3, pp. 2385–2403, 2019.

[13] P. H. Shah and B. R. Bhalja, "A new rate of change of impedance-based islanding detection scheme in presence of distributed generation," *Electr. Power Compon. Syst.*, vol. 42, no. 11, pp. 1172–1180, 2014.

[14] K. Sareen, B. R. Bhalja, and R. P. Maheshwari, "Universal islanding detection technique based on rate of change of sequence components of currents for distributed generations," *IET Renewable Power Gener.*, vol. 10, no. 2, pp. 228–237, 2016.

[15] D. Reigosa, F. Briz, C. Blanco, P. García, and J. M. Guerrero, "Active islanding detection for multiple parallel-connected inverter-based distributed generators using high-frequency signal injection," *IEEE Trans. Power Electron.*, vol. 29, no. 3, pp. 1192–1199, 2013.

[16] B. K. Choudhury and P. Jena, "A digital lock-in amplifier assisted active islanding detection technique for dc microgrids," *IEEE Trans. Ind. Appl.*, vol. 59, no. 1, pp. 377–391, 2022.

[17] D. Velasco, C. Trujillo, G. Garcerá, and E. Figueres, "Review of anti-islanding techniques in distributed generators," *Renewable Sustainable Energy Rev.*, vol. 14, no. 6, pp. 1608–1614, 2010.

[18] D. Mlakić, H. R. Baghaee, and S. Nikolovski, "A novel anfis-based islanding detection for inverter-interfaced microgrids," *IEEE Trans. Smart Grid*, vol. 10, no. 4, pp. 4411–4424, 2018.

[19] P. Kundur, "Power system stability," *Power Syst. Stab. Control*, vol. 10, pp. 7–1, 2007.

[20] X. Chen and Y. Li, "An islanding detection algorithm for inverter-based distributed generation based on reactive power control," *IEEE Trans. Power Electron.*, vol. 29, no. 9, pp. 4672–4683, 2013.

[21] J. Laghari, H. Mokhlis, A. H. A. Bakar, M. Karimi, and A. Shahriari, "An intelligent under frequency load shedding scheme for islanded distribution network," in *2012 IEEE Int. Power Eng. Optim. Conf. Melaka, Malaysia*, pp. 40–45, IEEE, 2012.

[22] H. Karimi, A. Yazdani, and R. Iravani, "Negative-sequence current injection for fast islanding detection of a distributed resource unit," *IEEE Trans. Power Electron.*, vol. 23, no. 1, pp. 298–307, 2008.

[23] L. Shi and F. Wu, "An islanding detection algorithm based on fuzzy adaptive phase drift control," in *2013 IEEE Int. Conf. Inf. Autom. (ICIA)*, pp. 225–229, IEEE, 2013.

[24] H. Vahedi and M. Karrari, "Adaptive fuzzy sandia frequency-shift method for islanding protection of inverter-based distributed generation," *IEEE Trans. Power Delivery*, vol. 28, no. 1, pp. 84–92, 2012.

[25] K. Narayanan, S. A. Siddiqui, and M. Fozdar, "Hybrid islanding detection method and priority-based load shedding for distribution networks in the presence of dg units," *IET Gener. Transm. Distrib.*, vol. 11, no. 3, pp. 586–595, 2017.

[26] J. A. Laghari, H. Mokhlis, A. Bakar, and M. Karimi, "A new islanding detection technique for multiple mini hydro based on rate of change of reactive power and load connecting strategy," *Energy Convers. Manage.*, vol. 76, pp. 215–224, 2013.

[27] L. Ganyun, C. Haozhong, Z. Haibao, and D. Lixin, "Fault diagnosis of power transformer based on multi-layer svm classifier," *Electr. Power Syst. Res.*, vol. 74, no. 1, pp. 1–7, 2005.

[28] L. Breiman, "Random forests," *Mach. Learn.*, vol. 45, pp. 5–32, 2001.

[29] G. Song, B. Cao, and L. Chang, "A passive islanding detection method for distribution power systems with multiple inverters," *IEEE J. Emerging Sel. Top. Power Electron.*, vol. 10, no. 5, pp. 5727–5737, 2022.